# The MR Appearance of CSF Flow in Patients with Ventriculomegaly

John L. Sherman, Charles M. Citrin, Raymond E. Gangarosa and Bruce J. Bowen

*AJNR Am J Neuroradiol* 1986, 7 (6) 1025-1031
http://www.ajnr.org/content/7/6/1025

# The MR Appearance of CSF Flow in Patients with Ventriculomegaly

John L. Sherman[1-3]
Charles M.Citrin[1, 3]
Raymond E. Gangarosa[4]
Bruce J. Bowen[1]

**The purpose of this study was to investigate the MR imaging appearance of mobile CSF in the ventricular system in patients with ventriculomegaly caused by brain atrophy and extraventricular obstructive hydrocephalus. Pulsatile CSF often has decreased intensity relative to less mobile areas of CSF, particularly on T2-weighted scans. At times, the flow-related signal dropout causes striking heterogeneity in the appearance of CSF. This has been termed the *CSF flow-void sign* (CFVS) and is most likely caused by spin-phase shifts and time-of-flight effects created as a result of CSF turbulence and increased velocity of CSF pulsatile flow. The effect is most pronounced in areas where a larger volume of CSF moves through a small channel or foramen, such as the aqueduct of Sylvius or foramen of Magendie. The scans of 40 patients with ventriculomegaly caused by brain atrophy or extraventricular obstructive hydrocephalus were reviewed for the presence of the CFVS. All patients had the CFVS in the aqueduct of Sylvius on T2-weighted spin-echo sequences. The sign was present in the fourth ventricle in 96%, in the third ventricle in 70%, in the foramen of Magendie in 65–77%, and in the foramina of Monro in 33%. The sign was more pronounced in patients with larger ventricles but could not be used to differentiate patients with brain atrophy from those with extraventricular obstructive hydrocephalus.**

MR imaging has proven superior to CT in the evaluation of intracranial disease primarily because of its superior contrast resolution [1–3]. Cerebral vasculature and vascular malformations are clearly delineated by hypointensity resulting from the lack of signal caused by rapidly flowing blood [4, 5]. Rapidly flowing or turbulent CSF in the third ventricle, the aqueduct of Sylvius, and the fourth ventricle may also be delineated as a hypointense area because of the lack of signal (Fig. 1). This has been termed the *CSF flow-void sign* (CFVS) [6, 7]. We investigated the incidence and variations of the CFVS in patients with ventriculomegaly caused by brain atrophy and extraventricular obstructive hydrocephalus (EVOH) [8].

## Materials and Methods

The MR examinations of 40 patients with enlarged ventricles were reviewed and divided into two groups on the basis of clinical evaluations and results of other imaging studies. Patients with evidence of obstruction or mass effect involving the third ventricle, fourth ventricle, or aqueduct of Sylvius were excluded.

Group 1 included 29 patients with enlarged ventricles caused by brain atrophy, normal aging, or congenital anomalies. There were 19 men and 10 women aged 17–83 years (average age, 57 years). Two patients were 17 years old: between them, one had vermian dysgenesis and the other had olivopontocerebellar degeneration.

Group 2 included 11 patients with EVOH. The five males and six females were 2–77 years old (average age, 56 years). One patient (a 36-year-old man) had presumed inferior vermian dysgenesis but also had EVOH from previous head trauma.

All examinations were evaluated for the presence of the CFVS [6] on T2-weighted images and on T1-weighted images or balanced T2/T1 images. The CFVS was differentiated from the low signal intensity of arteries and veins by comparing the size and location of the sign

**This article appears in the November/December 1986 issue of AJNR and the January 1987 issue of *AJR*.**

Received March 3, 1986; accepted after revision May 28, 1986.

Presented in part at the annual meeting of the Radiological Society of North America, Chicago, November 1985.

[1] Magnetic Imaging of Washington, 5550 Friendship Blvd., Chevy Chase, MD 20815. Address reprint requests to J. L. Sherman.

[2] Department of Radiology, Uniformed Services University of the Health Sciences, Bethesda, MD 20814.

[3] Department of Radiology, George Washington University School of Medicine, Washington, DC 20037.

[4] Clinical Science Center, Picker International, Highland Heights, OH 44143.

***AJNR* 7:1025–1031, November/December 1986**
0195–6108/86/0706–1025

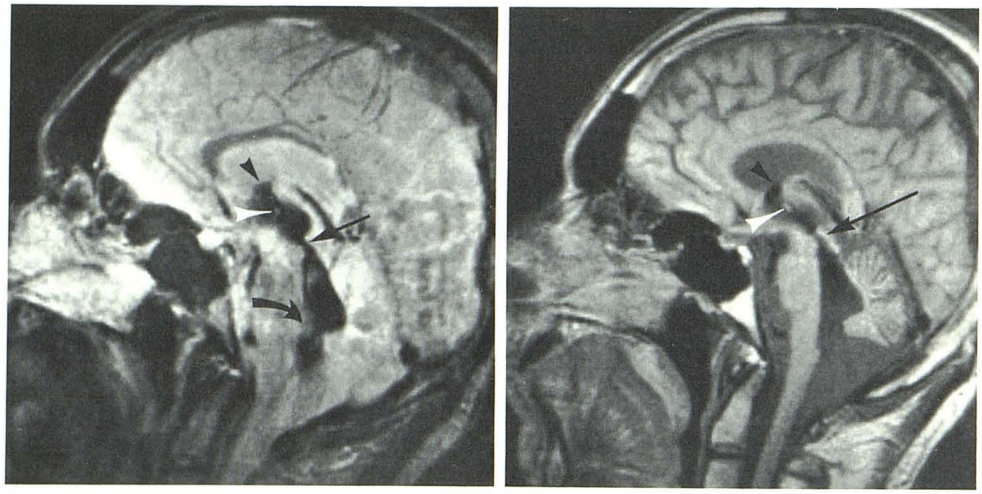

A B

Fig. 1.—37-year-old man with inferior vermian dysgenesis and posttraumatic EVOH. Basilar subarachnoid spaces are enlarged. Midsagittal MR scans are 5 mm thick. **A**, T2-weighted scan (SE 2200/80). CSF in lateral ventricles is bright. Striking CFVS in foramina of Monro (*black arrowhead*), third ventricle, aqueduct of Sylvius (*straight arrow*), fourth ventricle, and foramen of Magendie (*curved arrow*). CFVS surrounds massa intermedia (*white arrowhead*). **B**, T1-weighted scan (SE 750/40). CFVS is less well seen but is present in foramina of Monro (*black arrowhead*), posterior third ventricle, aqueduct of Sylvius (*arrow*), and proximal fourth ventricle. Massa intermedia (*white arrowhead*).

with known vascular anatomy. Its location was identified at the foramen of Magendie, the fourth ventricle, the aqueduct of Sylvius, the third ventricle, or at the foramina of Monro. The severity of the ventriculomegaly was measured using the ventricular size index [9], which is the ratio of the distance between the lateral margins of the frontal horns to the distance between the inner tables of the skull at the same level. Using this index, normal ventricular size is present when the ratio is 30% or less, mild ventriculomegaly is present with a ratio of 30–39%, moderate ventriculomegaly is present with a ratio of 40–46%, and severe ventriculomegaly is present with a ratio of 47% or more. (The same criteria were used in the "normal" group included in Table 2 reported by Sherman and Citrin [6].) The presence or absence of interstitial edema was also noted. The length of the longest unbroken CFVS was measured on the T2-weighted images.

MR examinations were performed with a Picker Vista MR superconductive 0.5-T imager with standard pulse sequences, software, and hardware. Read gradient magnetic field amplitudes used in these sequences were $3 \times 10^{-3}$ T/m. Data were typically acquired with 256 complex samples/view, 256 views, and two excitations using the standard 2DFT method and spin-echo (SE) pulse sequences [10]. Magnitude reconstruction was used in all cases. The resultant 256 × 256 image was then interpolated to a 512-element display matrix. Field of view for these examinations was 30 cm, resulting in a pixel size before interpolation of 1.17 mm. Sampling times were 24 msec, and sampling bandwidth 5 kHz. The phase-encoding gradient was in the horizontal plane for all cases. Single-echo 8- or 16-multisection SE sequences were performed with selective excitation in staggered slice order by exciting odd-numbered slices sequentially followed by even-numbered slices sequentially. Slices were contiguous and either 5 or 10 mm thick. Slice profiles were approximately trapezoidal, with 1 mm transitional zones on either side of a flat region of the nominal thickness [11]. T2-and T1-weighted sequences were used in all cases.

T2-weighted sequences were obtained with a TE of 60, 80, or 100 msec and a TR of 1500–4000 msec. T1-weighted sequences used a TE of 30 or 40 msec, with a TR of 500–600 msec. The CSF in the lateral ventricles appears hyperintense relative to cerebral cortex on the T2-weighted sequences and hypointense on the T1-weighted sequences. In some cases additional sequences were added to the basic examination. Slice-to-slice variability in contrast was not significant in any pulse sequences.

## Results

Sixteen patients (40%) had mild ventriculomegaly, 15 (37%) had moderate ventriculomegaly, and nine (23%) had severe ventriculomegaly. The occurrence of the CFVS in patients with brain atrophy or EVOH is given in Table 1. The CFVS was more difficult to identify specifically in the foramen of Magendie in five patients because of the proximity of the posterior inferior cerebellar arteries.

### *Group 1: Ventriculomegaly from Atrophy or Congenital Anomaly*

Fifteen of these 29 patients had mild ventriculomegaly, 10 had moderate enlargement, and four had severe enlargement of the ventricles. Two patients had a periventricular rim of slightly increased intensity that was believed to represent deep white-matter disease, probably caused by ischemia.

TABLE 1: **CFVS Occurrence in Atrophy and Extraventricular Obstructive Hydrocephalus (EVOH)**

| Location of CFVS | No. of Patients (%) | | |
|---|---|---|---|
| | Cerebral Atrophy ($n$ = 29) | EVOH ($n$ = 11) | Total ($n$ = 40) |
| Foramen of Monro | 8 (28) | 5 (45) | 13 (33) |
| Third ventricle | 19 (66) | 9 (82) | 28 (70) |
| Aqueduct | 29 (100) | 11 (100) | 40 (100) |
| Fourth ventricle | 27 (93) | 11 (100) | 38 (95) |
| Foramen of Magendie* | 17–21 (59–72) | 9–10 (82–91) | 26–31 (65–78) |
| CFVS length (average) | 37 mm | 47 mm | 40 mm |

Note.—CSF flow-void sign (CFVS) was analyzed on MR images obtained with T2-weighted spin-echo pulse sequences (TR = 1500–4000 msec, TE = 60–100 msec).

* Range of observations reflects the difficulty in separating the CFVS from arterial structures.

TABLE 2: **CFVS Occurrence According to Ventricular Size**

| Location of CFVS | Degree of Ventriculomegaly and No. of Patients (%) | | | |
|---|---|---|---|---|
| | Normal ($n$ = 46) | Mild ($n$ = 16) | Moderate ($n$ = 15) | Severe ($n$ = 9) |
| Foramen of Monro | 0 | 4 (24) | 5 (27) | 5 (56) |
| Third ventricle | 2 (4) | 10 (63) | 11 (73) | 7 (78) |
| Aqueduct | 31 (67) | 16 (100) | 15 (100) | 9 (100) |
| Fourth ventricle | 15 (32) | 15 (94) | 14 (93) | 9 (100) |
| Foramen of Magendie* | 18 (39) | 8–11 (50–67) | 11–13 (73–87) | 7 (78) |

Note.—Data were compiled on the visualization of the CSF flow-void sign (CFVS) on T2-weighted spin-echo pulse sequence (TR = 1500–4000 msec, TE = 60–100 msec). Data on normal patients from [6]. Categorization of ventricular size was made during the ventricular size index. Note the increasing likelihood of observing the CFVS as ventricular size increases.

* Range of observations reflects the difficulty in separating the CFVS from arterial structures.

All 29 patients had the CFVS in the aqueduct of Sylvius on T2-weighted images. One patient with severe ventriculomegaly had a narrow CFVS in the aqueduct and mild periventricular hyperintensity. Before the MR examination, this patient was suspected of having aqueductal stenosis; however, a limited pneumoencephalogram showed free passage of air into the third ventricle. A radionuclide cisternogram was normal. Nineteen patients (66%) had the sign in the third ventricle and 27 (93%) had the sign in the fourth ventricle. Of the 27 patients with CFVS in the fourth ventricle, 17 to 21 (59–72%) had the sign in the foramen of Magendie. Eight patients (28%) had the CFVS in or near the foramina of Monro. Twenty-six patients (90%) had the CFVS on T1-weighted images. In these cases it was seen only in areas that were positive for the CFVS on the T2-weighted images. The average length of the CFVS was 3.7 cm.

*Group 2: EVOH*

One of these 11 patients had mild hydrocephalus, while five had moderate hydrocephalus and five had severe hydrocephalus. Three of the patients with moderate and two with severe hydrocephalus had a smooth periventricular rim of increased intensity on T2-weighted images that was interpreted as interstitial edema. The CFVS was most marked in the patient with inferior vermian dysgenesis and moderate hydrocephalus (Fig. 1).

All patients had the CFVS in the aqueduct of Sylvius and fourth ventricle on T2-weighted scans. Nine or 10 (82–91%) of these patients had the sign clearly in the foramen of Magendie, while it was absent in this location in two others. Nine patients (82%) had the CFVS in the third ventricle and five (45%) had the CFVS in or near the foramina of Monro. Ten patients (91%) had evidence of the CFVS on T1-weighted images in areas also positive for the CFVS on T2-weighted images. The average length of the CFVS was 4.7 cm.

The data are summarized in Table 1. An analysis of the data according to ventricular size has been combined with previously reported observations of the CFVS in normal patients [6] and is presented in Table 2.

## Discussion

The forces driving CSF throughout the subarachnoid space are not completely understood. The rate of continuous formation (0.4 ml/min) and absorption of CSF is inadequate to produce flow velocities detectable by MR. However, turbulence and localized areas of high-velocity CSF flow are created by pulsatile shifts of CSF. These CSF pulsations have been commonly observed during Pantopaque myelography or cisternography. In 1943, O'Connell [12] suggested that intrancranial arterial pulsations were the main source of CSF pulsations. In 1955, Bering [13] maintained that the main impetus to CSF pulsations was pulsations within the choroid plexus. In 1966, Du Boulay [14] confirmed O'Connell's theoretical concepts, showing that forceful CSF pulsations occur in the basilar subarachnoid space and third ventricle in synchrony with arterial systole and diastole. He referred to the forceful thalamic compression of the third ventricle as the "third ventricular pump" and discounted the contribution of choroid plexus pulsation. Du Boulay believed that pulsation in the basal cisterns stemmed from displacement of CSF from the brain as well as expansion of the main arteries in the basilar cisterns.

Flow-dependent effects in the presence of magnetic field gradients have been described in conventional [15], specialized [16], and zeugmatographic [17, 18] MR devices. Flow-dependent MR images have been shown in both conventional [19] and specialized pulse sequences [20]. These effects can be manifested as time-of-flight or phase-shift effects, or as a combination of both, as is the case in conventional 2DFT SE sequences [16, 21]. Time-of-flight effects include flow-related enhancement (as seen in slow venous flow) and high-velocity signal loss, which occurs with rapid flow (10 cm/sec or more) caused by movement of spins out of the imaged volume before the refocusing pulses occur [22]. As von Schulthess and Higgins [21] pointed out, this effect may explain the loss of signal for flow of spins perpendicular to the plane, but it cannot explain loss of signal for flowing spins coursing within the imaged plane. Spin-phase shifts occur whenever spins move in gradient fields regardless of whether the movement is in the imaged plane. In the case of spins flowing along a magnetic gradient, the magnetic field experienced by those spins varies during the evolution of the pulse sequence. Thus, the magnetic history of the spins will be more complex in the case of flowing spins. The signal intensity is critically dependent on the spatial distribution of velocities and accelerations of spins within a voxel. The larger the spatial variation of the velocity or accelerations across a voxel, the greater the loss in signal amplitude [18]. Turbulence, whether from high velocity or intrinsic physiologic movements, results in large spatial variations of the velocities of the fluid within the imaging plane that then translate into spin-phase changes and loss of signal

amplitude. We have anecdotally noted that the CFVS is present in the aqueduct on both odd and even echoes, in keeping with von Schulthess and Higgins' observations on spin-phase changes in blood vessels. Changes in the phase-encoding plane have not been noted to change the CFVS, although associated artifacts are moved from one plane to the other. Based on the above observations, most of the aqueductal signal loss known as the aqueductal CFVS is most likely caused by spin-phase changes. These observations do not necessarily apply to the loss of signal in other subarachnoid spaces. For example, we have noted more uniform signal intensity in the spinal CSF on the second echo of a multiecho chain. Theoretically, the time-of-flight effects could be calculated by determining the differences in intensity between images of identical TR and TE on single-echo images versus dual-echo images. We recently presented material confirming the relation of the CFVS to the cardiac cycle, specifically showing more marked loss of signal (CFVS) during cardiac systole [23], apparently because of accentuation of the time-of-flight effects. Similar effects may be seen from fortuitous synchronization of the cardiac cycle and the MR acquisition sequence. This has been termed "pseudogating" [22] and could be a factor in some instances [24].

A comparison of the reported incidence of the CFVS in patients with normal ventricles [6] with those of our series indicates that it is seen much more often in patients with ventriculomegaly (Table 2). Our results indicate that the CFVS is present in the aqueduct of Sylvius in all patients with enlarged ventricles caused by brain atrophy or EVOH (Figs. 1, 2, and 4). On T2-weighted images the CFVS stands out as an area of decreased intensity in contrast to the bright appearance of the CSF in other areas of the ventricular system (Figs. 1 and 2A). It was seen in the fourth ventricle in 96% of patients (Figs. 1–3), in the third ventricle in 70% (Figs. 1, 2, 4, and 5), in the foramina of Monro in 33% (Figs. 1, 2, and 5), and in the foramen of Magendie in 65–77% (Figs. 1–4). It was present in at least one area on T1-weighted scans in 90% of patients (Fig. 1B).

Subtle differences in CSF velocity or turbulence in different areas of the ventricle can be appreciated by comparing midsagittal T1-weighted images with midsagittal T2-weighted images in the same patient.

There is no difficulty in differentiating the CFVS in the aqueduct of Sylvius, third ventricle, or fourth ventricle from arteries or veins. However, care must be taken to differentiate the posterior inferior cerebellar arteries from the foramen of Magendie and the internal cerebral veins from the foramina of Monro (Figs. 2, 3, and 5). In these areas we relied on the size of the CFVS and close observations of the anatomy on contiguous sections. The CFVS probably occurs frequently in basilar cisterns but is more difficult to differentiate from vessels [7]. In one patient with brain atrophy and multiple sclerosis we observed large areas of decreased intensity that we believe represented the CFVS in the ambient cisterns (Fig. 6).

The CFVS was seen more often and was more prominent in the group of patients with EVOH (Table 1), but this is believed to be a reflection of the more marked ventricular enlargement in this group of patients. The data in Table 2 reflect the relatively frequent occurrence of the CFVS in the foramina of Monro, the third ventricle, the fourth ventricle, and the foramen of Magendie in moderate or severe ventricular enlargement when compared with only mild ventriculomegaly. The CFVS alone cannot be used to differentiate patients with brain atrophy from those with EVOH.

The increased frequency and prominence of the CFVS in patients with large ventricles is probably related to several factors. Decreased compliance of periventricular tissues may allow increased transmission of pulsations to the ventricular system [25]. The expansion of the CSF spaces alone in a turbulent system may simply allow more mixing of spins with differing constant velocities and accelerations, resulting in more signal loss from spin-phase changes [21]. Signal loss from time-of-flight effects may also be increased in patients with large ventricles. These effects are most likely to be seen in areas where the cross-sectional area of the CSF space narrows abruptly, such as the aqueduct of Sylvius and the various ventricular foramina. Although the net production of CSF does not change, the velocity of CSF flow through these

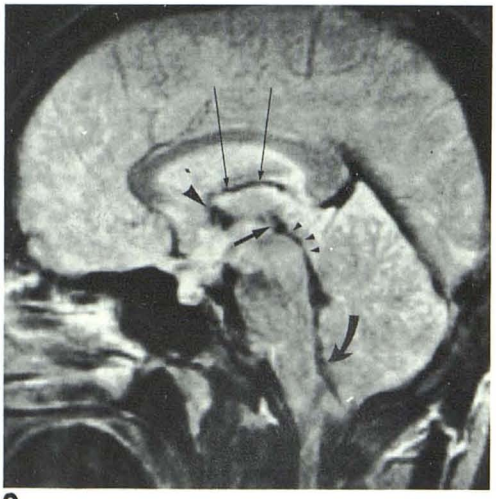

2

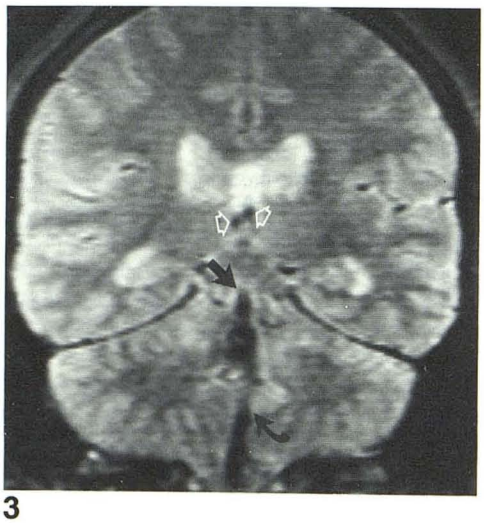

3

Fig. 2.—65-year-old man with mild cerebral atrophy. T2-weighted (SE 2200/80) midsagittal scan is 5 mm thick. CFVS in foramina of Monro (*large arrowhead*), third ventricle (*short straight arrow*), aqueduct of Sylvius (*small arrowheads*), fourth ventricle, and foramen of Magendie (*curved arrow*). Note proximity of internal cerebral veins to foramina of Monro (*long straight arrows*).

Fig. 3.—55-year-old man with mild cerebral atrophy. T2-weighted (SE 2400/80) coronal scan through plane of floor of fourth ventricle is 5 mm thick. Aqueduct of Sylvius (*straight solid arrow*), foramen of Magendie (*curved arrow*), internal cerebral veins (*open arrows*).

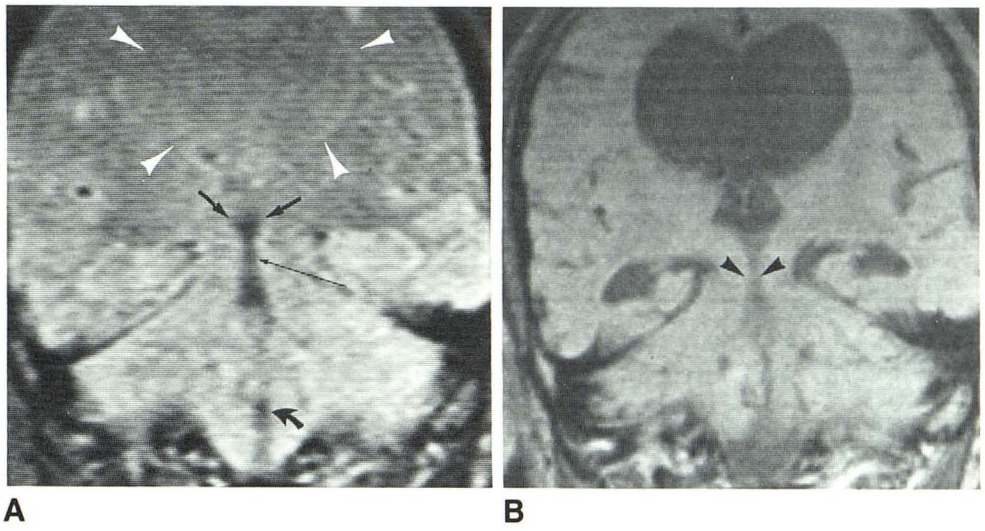

Fig. 4.—61-year-old man with EVOH. Fourth ventricle is small. Coronal scans through plane of aqueduct and fourth ventricle are 10 mm thick. **A**, T2-weighted scan (SE 1600/100). CSF in enlarged lateral ventricles is isointense with brain (*arrowheads*). CFVS in posterior third ventricle (*short straight arrows*), aqueduct of Sylvius (*long straight arrow*), rostral fourth ventricle, and foramen of Magendie (*curved arrow*), indicating patency of these areas. **B**, Balanced T2/T1 scan (SE 1500/40). Aqueduct of Sylvius (*arrowheads*) appears to be laterally compressed.

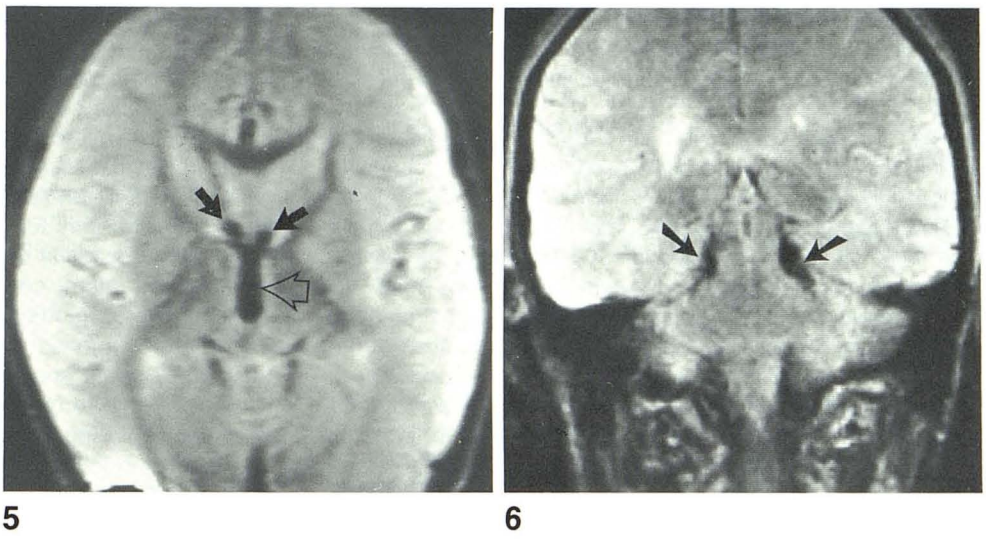

Fig. 5.—2-year-old girl with EVOH. T2-weighted (SE 2400/80) axial scan is 10 mm thick. CFVS is seen well in foramina of Monro (*solid arrows*) and in third ventricle (*open arrow*). Artifact from shunt tube is seen posteriorly on right side.

Fig. 6.—35-year-old woman with multiple sclerosis. T2-weighted (SE 2400/80) coronal scan through posterior brainstem is 5 mm thick. Prominent areas of decreased intensity in ambient cisterns (*arrows*) probably represent summation of CFVS and cerebral vasculature.

areas will be increased. This can be explained by applying the concept of the continuity equation [26], which states that for a steady-stream tube with a narrow end (section 1) and a wide end (section 2), the product of density (d), velocity (v), and cross-sectional area (A) is the same at both ends, or $d_1v_1A_1 = d_2v_2A_2$. The actual description of the flow through a structure such as the aqueduct of Sylvius is much more complex, but the concept is valid. In patients with hydrocephalus, the change in the cross-sectional area of the ventricles relative to the normal state is much greater than the change in the size of the aqueduct of Sylvius or the ventricular foramina relative to their normal state. Thus, applying the continuity equation, the velocity of the CSF flow must increase. This in turn could lead to high-velocity signal loss as well as spin-phase shift signal loss.

We cannot explain the smaller-than-expected aqueductal CFVS in one patient with severe hydrocephalus, but we were able to corroborate the pneumoencephalographic finding of aqueductal patency by using a 5-mm T2-weighted (SE 2300/80) MR imaging pulse sequence (Fig. 7). Mild stenosis of the caudal segment of the aqueduct may be present. This case is important since it illustrated the utility of the CFVS in the aqueduct. In future cases the observation of the CFVS in the aqueduct may obviate invasive techniques to evaluate the aqueduct. This case also illustrates the need to use meticulous technique. The narrow CFVS might not have been seen if there had been patient motion or if other factors decreased spatial and/or contrast resolution.

One patient had a marked CFVS extending from the foramina of Monro to the foramen of Magendie, virtually filling the fourth ventricle (Fig. 1). As in all cases, the CFVS was best seen on the T2-weighted sequence. This patient had inferior vermian dysgenesis and probable posttraumatic EVOH. The caudal aqueduct of Sylvius was dilated. The foramen of Magendie was voluminous and may have allowed more vigorous transmission of CSF pulsations into the fourth ventricle

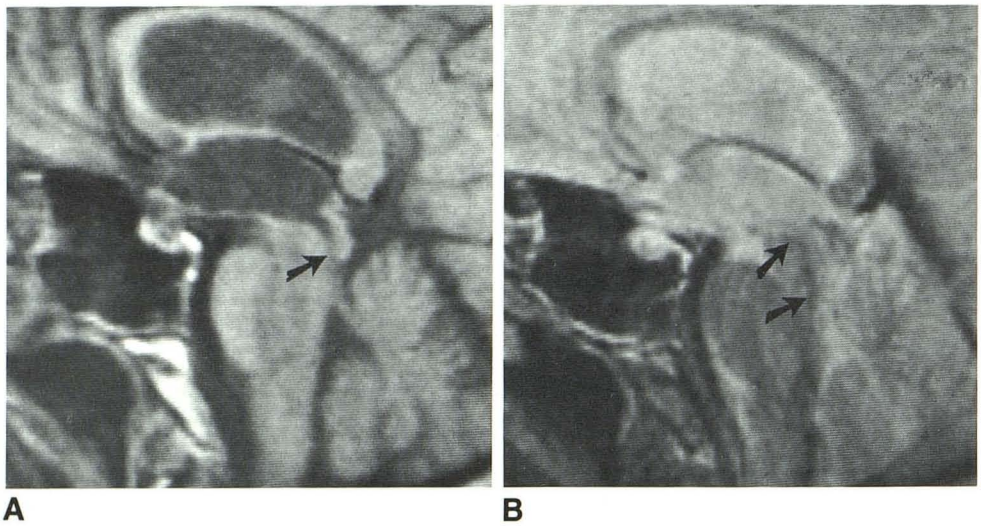

Fig. 7.—77-year-old man with cerebral atrophy. Midsagittal scans are 5 mm thick. **A**, T1-weighted (SE 750/40). Dilated lateral and third ventricles. Caudal segment of aqueduct of Sylvius is poorly seen (*arrow*). **B**, T2-weighted (SE 2300/80). CFVS is present (*arrows*), indicating patency of aqueduct of Sylvius. Limited pneumoencephalogram confirmed patency of aqueduct of Sylvius.

and aqueduct. It has been stated that the pulsatile displacement of CSF through the basal cisterns is 10 to 25 times as great as the ventricular displacement, even in normal patients [24, 27, 28].

The CFVS is a useful direct indicator of the patency of the channel or foramen in which it is seen. In 25–35% of patients with EVOH, the fourth ventricle is normal or minimally enlarged [29]. We encountered two such patients in our series (Fig. 4). The observation of the aqueductal CFVS avoids the consideration of aqueductal obstruction in those patients. The CFVS should prove to be more useful than the traditional criterion for determining the site of obstruction by observation of the point of transition from dilated to nondilated CSF spaces.

Magnetic field strength does not appear to be an important factor. The CFVS has been observed on a variety of systems at different field strengths including 0.35 T, 0.5 T, 0.6 T, and 1.5 T [6, 7, 24, 30]. We have also anecdotally observed the sign on images from a 0.3 T permanent magnet system. Von Schulthess and Higgins [21] suggested that the loss of signal from movements of spins in gradient fields (spin-phase changes) may vary between the different MR imager systems. This is because of the variability in gradient fields used for spatial position encoding. We are not aware of examples of such machine differences at this time.

We have noted a markedly higher incidence of the CFVS when comparing scans obtained with T2-weighted versus T1-weighted SE pulse sequences. Since the loss of signal is probably primarily from spin-phase changes, the phenomenon should not depend on the TE or TR. However, the decreased intensity will not be easily observed unless the intensity of the CSF is increased. The longer TE/TR sequences provide better contrast and thus allow easier detection of the CFVS. Time-of-flight effects are dependent on the TE and are more likely to be demonstrated as the TE increases [4].

The CFVS may prove to be useful in the follow-up examination of patients with treated (shunted) hydrocephalus. There have been reports of the development of shunt independence with spontaneous nonsurgical restoration of normal CSF circulatory patterns in 9–20% of patients treated for hydrocephalus [31–33]. The appearance of the CFVS in areas where it was previously absent would indicate restoration of normal CSF flow through the area. The disappearance of the CFVS in patients with hydrocephalus who are being followed should be of great value. It would be an indication that previously intact CSF flow pathways had been altered. For instance, some patients with EVOH have been shown to develop secondary aqueductal stenosis from depression of the third ventricle and lateral compression of the aqueduct by the enlarged lateral ventricle [34, 35]. This superimposes an obstructive component on an advanced EVOH and accelerates neurologic deterioration.

It is important to recognize the CFVS because it explains otherwise confusing areas of heterogeneous intensity in CSF spaces and it provides information about CSF dynamics. While it promises to be a useful sign in the evaluation of patients with ventriculomegaly, further investigations of the sensitivity and specificity of the sign are needed. Although our results indicate that the CFVS is present in the aqueduct of Sylvius in all patients with hydrocephalus, we must add a note of caution since this series is limited to only 40 patients. It does appear clear that the presence of the CFVS in and of itself does not indicate the presence of EVOH. The application of the CFVS is leading us to a deeper understanding of CSF circulatory system dynamics, and this in turn may lead to improved diagnosis and treatment of patients with CSF circulatory disorders.

## ACKNOWLEDGMENTS

We thank Mary Anne Thomas, Arlene Kisliuk, and Bari Weiner for help in image preparation and manuscript review.

## REFERENCES

1. Bradley WG, Waluch V, Yadley RA, Wycoff RR. Comparison of CT and MR in 400 patients with suspected disease of the brain

and cervical spinal cord. *Radiology* **1984**;152:695–702
2. Brant-Zawadzki M, David PL, Crooks LE, et al. NMR demonstration of cerebral abnormalities: comparison with CT. *AJNR* **1983**;4:117–124, *AJR* **1983**;140:847–854
3. Bydder GM, Steiner RE, Young IR, et al. Clinical NMR imaging of the brain: 140 cases. *AJNR* **1982**;3:459–480, *AJR* **1982**;139:215–236
4. Bradley WG, Waluch V, Laie K, Fernandez EJ, Spalter C. The appearance of rapidly flowing blood on magnetic resonance images. *AJR* **1984**;143:1167–1174
5. Kucharczyk W, Lemme-Pleghos L, Uske A, Brant-Zawadzki M, Dooms G, Norman D. Intracranial vascular malformations: MR and CT imaging. *Radiology* **1985**;156:383–389
6. Sherman JL, Citrin CM. Magnetic resonance demonstration of normal CSF flow. *AJNR* **1986**;7:3–6
7. DeLaPaz RL, Davis DO, Norman D, O'Donohue J, Enzmann DR. Cerebrospinal fluid motion effects in cerebral MR imaging. Presented at the annual meeting of the Radiological Society of North America, Chicago, November **1985**
8. Naidich TP, Schott LH, Baron RL. Computed tomography in the evaluation of hydrocephalus. *Radiol Clin North Am* **1982**;20:143–167
9. TerBrugge KG, Rao KC. Hydrocephalus and atrophy, In: Lee SH, Rao KC, eds. *Cranial computed tomography*. New York: McGraw-Hill, **1983**:171–200
10. Haacke EM, Bearden FH, Clayton JR, Linga NR. Reduction of MR imaging time by the hybrid fast-scan technique. *Radiology* **1986**;158:521–529
11. Chui KM, Blakesley DM, Mohapatra SN. Test method for MR image slice profile. *J Comput Assist Tomogr* **1985**;9:1150–1152
12. O'Connell JEA. The vascular factor in intracranial pressure and the maintenance of the cerebrospinal fluid circulation. *Brain* **1943**;66:204–228
13. Bering EA. Choroid plexus and arterial pulsation of the choroid plexuses as a cerebrospinal fluid pump. *Arch Neurol Psychiatry* **1955**;73:165–172
14.; Du Boulay GH. Pulsatile movements in the CSF pathways. *Br J Radiol* **1966**;39:255–262
15. Singer JR. Blood flow rates by nuclear magnetic resonance measurements. *Science* **1985**;130:1652–1653
16. Battocletti JH, Linehan JH, Larsen SJ, et al. Analysis of a nuclear magnetic resonance blood flow for pulsatile flow. *IEEE Trans Biomed Eng* **1972**;19:403–407
17. Moran PR. A flow velocity zeugmatographic interlace for NMR imaging in humans. *Magnetic Resonance Imaging* **1982**;1:197–203
18. Waluch V, Bradley WG. NMR even echo rephasing in slow laminar flow. *J Comput Assist Tomogr* **1984**;8:594–598
19. Wedeen VJ, Meuli RA, Edelman RR, et al. Projective imaging of pulsatile flow with magnetic resonance. *Science* **1985**;230:946–948
20. Le Bihan D, Breton E, Lallemand D, Grenier P, Cabanis E. Diffusion MR imaging: neurological results. Presented at the annual meeting of the Radiological Society of North America, Chicago, November **1985**
21. von Schulthess GK, Higgins CR. Blood flow imaging with MR: spin-phase phenomena. *Radiology* **1985**;157:687–695
22. Bradley WG, Waluch VW. Blood flow: magnetic resonance imaging. *Radiology* **1985**;154:443–450
23. Citrin CM, Sherman JL. Alteration of the MRI appearance of CSF flow by cardiac gating. Presented at the annual meeting of the American Society of Neuroradiology, San Diego, January **1986**
24. Bradley WG, Kortman KE. Use of aqueductal flow void phenomenon in the diagnosis of normal pressure hydrocephalus. Presented at the annual meeting of the American Society of Neuroradiology, San Diego January **1986**
25. Bradley WG, Kortman KE. Use of the aqueductal flow void phenomenon in the diagnosis of normal pressure hydrocephalus. Presented at the annual meeting of the American Society of Neuroradiology, San Diego, January **1986**
26. Streeter VL. *Fluid mechanics*. 6th ed. New York: McGraw-Hill, **1975**:134–144
27. Du Boulay GH. Specialization broadens the view. The significance of a C.S.F. pulse. *Clin Radiol* **1972**;23:401–409
28. Du Boulay GH, Shah SH, Currie JC, Logue V. The mechanism of hydromyelia in Chiari type 1 malformations. *Br J Radiol* **1974**;47:579–587
29. Naidich TP, Schott LH, Baron BL. Computed tomography in the evaluation of hydrocephalus. *Radiol Clin North Am* **1982**;20:143–167
30. Mills CM, Posin JP, McCreary J, Kleiner BC. MRI of the spine: effect of flow on CSF intensity. Presented at the annual meeting of the American Society of Neuroradiology, San Diego, January **1986**
31. Johnston IH, Howman-Giles R, Whittle IR. The arrest of treated hydrocephalus in children. *J Neurosurg* **1984**;61:752–756
32. Hemmer R, Bohm B. Once a shunt, always a shunt? *Med Child Neurol* **1976**;18[suppl 37]:69–73
33. Holtzer GJ, de Lange SA. Shunt-independent arrest of hydrocephalus. *Neurosurgery* **1972**;39:698–701
34. Nugent GR, Al-Mefty O, Chou S. Communicating hydrocephalus as a cause of aqueductal stenosis. *J Neurosurg* **1979**;51:812–818
35. McMillan JJ, Williams B. Aqueduct stenosis: case review and discussion. *J Neurol Neurosurg Psychiatry* **1977**;40:521–532